Contents

Chapter 1

Cyclotron

In addition to the cyclotron accelerator, this first chapter introduces preliminary beam optics notions, including orbit, field index, periodic stability, optical functions, together with a key optical element: the dipole magnet. These concepts will be manipulated throughout the course. The chapter also familiarizes with raytracing and computer program simulations, starting with short, simple, optical sequences.

1.1 Introduction

The cyclotron arrived at a time, ∼1930 [1] (Fig. 1.1), where techniques to accelerate ions were sought, for the study of nuclear properties of the atom. To this day, hundreds of cyclotrons have been built, and more still are, to accelerate protons, ions, radioactive isotopes. They find application in "particle factories" (production of high flux beams of muons, neutrons, etc., Fig. 1.2), protontherapy (Fig. 1.3), production of radio-isotopes for medicine, and more. Cryogeny technologies allow further progress towards compactness (Fig. 1.3), and towards higher rigidities [2] (Fig. 1.4).

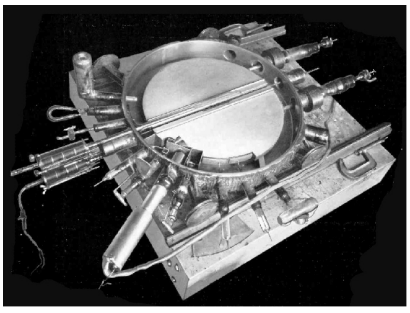

Fig. 1.1 An early cyclotron, late 1930s.

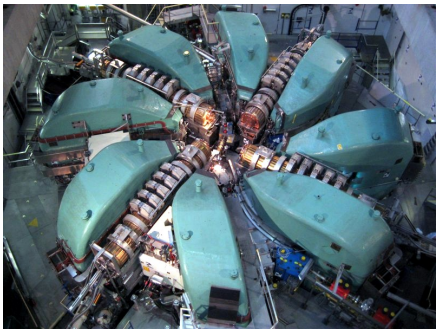

Fig. 1.2 The high power CW proton cyclotron at PSI, 1.4 MW today steadily increasing with years. It delivers a 590 MeV beam for secondary particle production (*e.g.*, neutron, muon).

The cyclotron combined together two long known concepts: resonant acceler-

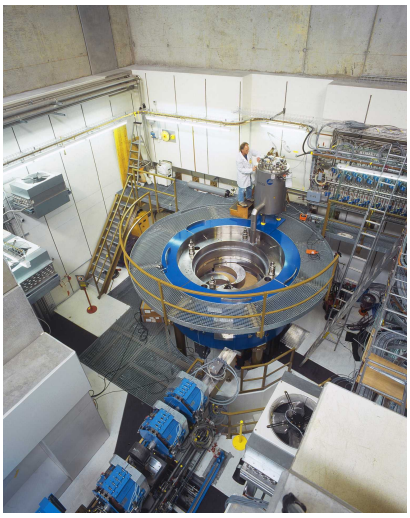

Fig. 1.3 Superconducting-coil isochronous spiral-sector AVF cyclotron at PSI, providing 250 MeV, 500 nA beams for hadrontherapy.

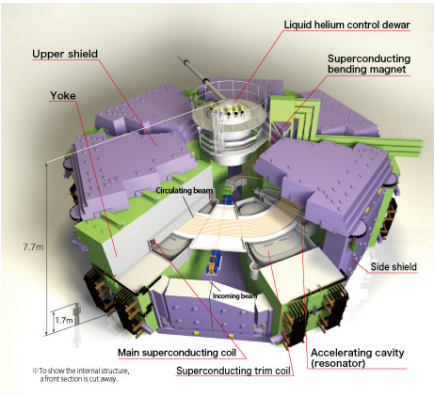

Fig. 1.4 RIKEN superconducting-coils separated-sector K*** heavy ion cyclotron, a compact, ∼ 20 m diameter, K-***, *** GeV proton equivalent rigidity [2].

ation through electric gaps, and trajectory bending by a magnetic field. It was conceived as a means to overcome the inconvenient of using a long series of high voltage electrodes in a linear layout, by, instead, repeated recirculation using a magnetic field, for incremental, resonant, energy gain through a single accelerating gap. This gap is formed by a pair of cylindrical electrodes, the "dees" (Figs. 1.5). which are applied a fixed frequency oscillating voltage, generated using a radio transmitter. The dees are plunged in a uniform magnetic field which causes the ion bunches to follow, as they are accelerated, a piecewise-circular path with increasing radius, normal to the field, in synchronism with the voltage oscillation. Here lies

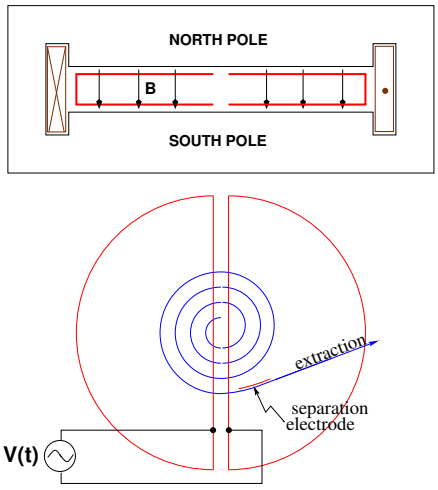

Fig. 1.5 Cyclotron : trajectories spiral in the uniform magnetic field between two circular poles. A double-dee forms a gap which is applied an oscillating voltage V(t) with frequency an integer multiple h of the revolution frequency, causing particles with the proper phase with respect to V(t) to be accelerated at each crossing. Bunch extraction is obtained by way of a separation electrode, located in the region etween the last two turns. *In passing: check the consistency of the coil current, direction of* $\vec{B}$ *and particle rotation - what is the sign of the accelerated particles?*

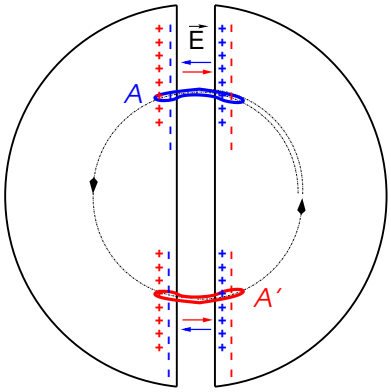

Fig. 1.6 Resonant acceleration: a bunch meeting an accelerating field $\vec{E}$ across the gap at A, at time t, will meet again, half a revolution later, at time $t + T_{rev}/2 = t + hT_{rf}/2$, an accelerating field $\vec{E}$ across the gap at A', and so forth turn after turn.

the cyclotron idea: while an accelerated bunch spirals outward, the increase in the distance it travels over a turn is compensated by its velocity increase: in the non-relativistic approximation ($\gamma \approx 1$), the revolution time T_{rev} remains quasi-constant; with the appropriate voltage frequency $f_{rf} \approx h/T_{rev}$ revolution motion and RF can be maintained in close synchronism, Trev $\approx hT_{rf}$, so that the bunch transit the accelerating gaps during the accelerating phase of V(t) (Fig. 1.6).

A common method for a realistic modeling of the magnetic field of a cyclotron dipole magnet is to use a field map. Using a mathematical model is also a reasonable approach in a preliminary design phase, in particular it brings flexibility to tweak parameters such as field homogeneity, radial or azimuthal field dependence. These two techniques are employed in the exercises to come.

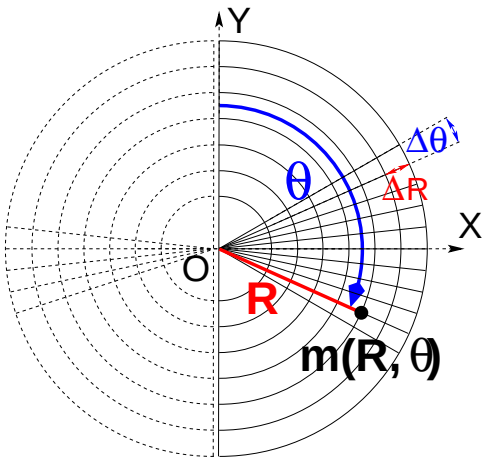

Fig. 1.7 A sketch of a cylindrical field map mesh, *i.e.*, a set of $m(R, \theta)$ nodes in a frame (O, X, Y), covering 180^0 (solid lines). The median plane field map so defined, namely the set of vertical field component values $B_Z(R, \theta)$ at the nodes of the mesh, represents a half of the cyclotron dipole; using it twice (additional 180^0 dashed line mesh) allows covering the all 360^o dipole. The mesh nodes are distant ΔR radially, $\Delta\theta$ in angle. Note: fabricating a 2D median plane field map is an easy way to define a magnetic field distribution for raytracing, often useful when an accurate analytical modeling is not available at hand.

• **Exercise 1.1-1.** *Model a magnet using a field map; raytrace using that field map model; check geometrical and dynamical outcomes against theory.*
Note 1: The optical sequence in zgoubi, for this exercise, is given in appendix 1.5.1 It uses (see *Zgoubi Users's Guide*), (i) `OBJET` to define a reference rigidity and to define the initial particle coordinates; (ii) `TOSCA` to read the field map and track

through step-by-step (and `TOSCA`'s '`IL=2`' flag to store step-by-step particle data into zgoubi.plt); (iii) `FAISCEAU` to print out particle coordinates in zgoubi.res, or `FAISTORE` to print out in *e.g.* zgoubi.fai.

Note 2: A short fortran program that generates the 180^o field map needed, is given in App. 1.5.1.

a - Construct a 180-degree 2-dimensional map of the field $B(R,\theta)$ in the plane located half-way between the north and south poles in Fig. 1.5. (the "median plane"). Use a uniform mesh in a cylindrical coordinate system (R,θ), covering R=1 to 76 cm. Zgoubi requires a reference radius as part of the field map data, a convenient value is $R_M = 50$ cm. The radial increment of the mesh is $\Delta R = 0.5$ cm, the axial increment is $\Delta\theta = 0.5$ cm/RM. Take constant axial field B = 0.5 T. The storage file, to be read by the tracking code, will have the following formatting, 6 columns:

$$R\cos\theta,\ Z,\ R\sin\theta,\ BY,\ BZ,\ BX$$

with θ varying first, R varying second in that list. Z is the vertical direction (normal to the map mesh), $Z \equiv 0$.

b - Compute trajectories: for one turn, track a few protons on concentric trajectories centered on the center of the field map, ranging in $10 \leq R \leq 80$ cm (radius R and particle momentum $p = qB\rho$ shall have proper correlation for that, to be determined). Plot these concentric trajectories in the lab frame.

c - Plot the revolution time T_{rev} as a function of radius R and kinetic energy E_k (two abscissa axes). Superimpose the theoretical $T_{rev}(R)$ and $T_{rev}(E_k)$ curves. Explain what causes the slow increase of revolution period with energy. •

The difference between static field (conservative, *e.g.*, Cockcroft-Walton's) and time-varying field (non-conservative, cyclotron's - resonant) acceleration mechanisms:

It is not possible to accelerate a particle traveling on a closed path using an electrostatic field ($\tilde{E} = -\tilde{\mathrm{grad}}V(\tilde{R},t)$ derives from a scalar potential), as the work by $\vec{F} = q\vec{E}$ only depends on the initial and final states, it does not dependent on the path followed (Fig. 1.8):

$$W = \int_A^B \vec{F}.d\vec{s} = -q\int_A^B \vec{\mathrm{grad}}V.d\vec{s} = -q(V_B - V_A).$$

$$\text{On a closed path : } \oint \vec{F}.d\vec{s} = 0, \quad \text{conservative force, no work performed} \quad (1.1)$$

Consequence: a DC voltage gap in a circular machine does not yield energy gain. Instead, the work of a force of induction origin ($\tilde{E} = -\partial\tilde{A}/\partial t$ arises from the variation of a magnetic flux - $\tilde{B} = \tilde{\mathrm{rot}}\tilde{A}$, $\tilde{A}$ vector potential) may not be null on a closed path. This is achieved *for instance* using a radio-frequency system which feeds an oscillating voltage across a gap, $\hat{V}\sin(\omega_{rf}t + \phi)$ (Fig. 1.9). In the classical cyclotron the gap is formed mechanically by a double dee system (Fig. 1.5). In the separated sector cyclotron (Fig. 1.2) the accelerating system is an external resonant cavity inserted in the drift space between two magnets (in a similar manner as today's synchrotrons).

The quantities of concern, regarding orbital motion (R, $f_{rev} = \omega_{rev}/2\pi$), field

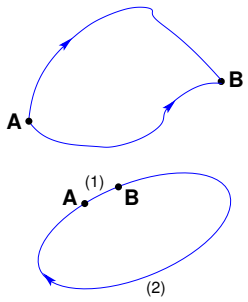

Fig. 1.8 The work of the electrostatic force only depends on V_A and V_B, independent of the path. In the case of the closed path: the particle loses along (2) the energy gained along (1).

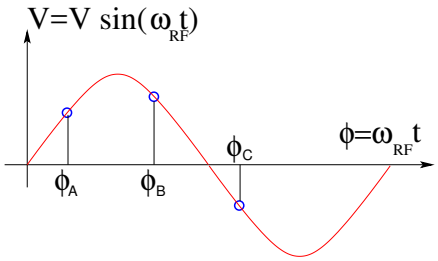

Fig. 1.9 A particle which reaches the gap at $\omega_{\rm rf}t = \phi_{\rm A}$ or $\omega_{rf}t = \phi_B$ is accelerated. If it reaches the RF gap at $\omega_{\rm rf}t = \phi_{\rm C}$ it is decelerated.

(B), satisfy

$$\mathrm{BR} = \mathrm{p/q}, \qquad 2\pi \mathrm{f_{rev}} = \mathrm{v/R} = \mathrm{qB/m} \tag{1.2}$$

These relationships hold whatever γ, from $v \ll c$ ($\gamma \approx 1$, domain of the *classical* cyclotron technology) to $\gamma > 1$ (domain of the *isochronous* cyclotron technology).

Note the first quantity introduced above, the *rigidity* of the particle of charge q and momentum p, BR = p/q, with R the curvature radius of the trajectory under the effect of the Laplace force in the field B. The *particle rigidity* is a quantity of predilection in accelerator physics and design, it will be omnipresent along these lectures.

The RF frequency $\mathrm{f_{rf}} = \omega_{\rm rf}/2\pi$ is constant in a cyclotron. In the isochronous cyclotron it satisfies $\mathrm{f_{rf}} = \mathrm{hf_{rev}}$ at a great accuracy, at all time (Sec. 1.3.3). In the classical cyclotron $\mathrm{f_{rf}}$ is set, by design, equal to $\mathrm{hf_{rev}}$ for an intermediate energy during the acceleration cycle, as the revolution time does vary (decreases) (Sec. 1.2.4).

The energy gain, or loss, by the particle when transiting the gap is

$$\Delta \mathrm{W} = \mathrm{q}\hat{\mathrm{V}} \sin\phi(\mathrm{t}) \quad \text{with } \phi(\mathrm{t}) = \omega_{\rm rf}\mathrm{t} - \omega_{\rm rev}\mathrm{t} + \phi_0 \tag{1.3}$$

with ϕ its phase with respect to the RF signal at the gap (*e.g.*, $\phi_{\rm A}$, $\phi_{\rm B}$ or ϕ_C in Fig. 1.9) and ϕ_0 the value at $t = 0$, $\omega_{\rm rev}$t the orbital angle of the particle.

• Exercise 1.1-2. *Modeling an accelerating gap, acceleration in a cyclotron.* Using the earlier 180^o field map and zgoubi input file, introduce an accelerating gap with peak voltage 100 kV: simulate it by means of `CAVITE[IOPT=3]`, and reproducing the configuration of Fig. 1.6.

a - Inject a proton with starting kinetic energy 200 keV (at the appropriate starting radius, $\mathrm{R_0} = \mathrm{p_0/qB}$, to be determined). Let it accelerate turn-by-turn through the gap (for multiturn, use `REBELOTE[NPASS=as many turns as needed; K=99]`, placed at the end of the sequence) until it reaches 6 MeV kinetic energy about. Plot the accelerated (spiraling out) trajectory all the way in a similar (O, X, Y) frame as in Fig. 1.7 (step-by-step particle data can be read from zgoubi.plt).

b - Plot the proton momentum pc and total energy E as a function of its kinetic energy, both from this numerical experiment (raytracing data stored using `FAISTORE`)

and from theory, everything on the same graph, use MeV units.
c - Plot the normalized velocity $\beta = \mathrm{v/c}$ as a function of kinetic energy, both numerical and theoretical, and in the latter case both classical and relativistic. •

• **Exercise 1.1-3.** *Accelerating to high energy, relativistic dynamics.*
Push the previous exercise to 3 GeV kinetic energy. For that, it will be necessary to extend the field map, to a maximum radius proper to encompass the spiraling trajectory up to 3 GeV. •

1.2 Classical cyclotron

Fixed-frequency acceleration requires the RF and cyclotron frequencies to be matched to one another. However the relativistic increase of the mass causes the revolution period to decrease with momentum, at a turn-by-turn rate of $\Delta \mathrm{T}/\mathrm{T_{rev}} = \gamma - 1$.

• **Exercise.** Give a theoretical demonstration of that relationship. •

The mis-match between the accelerating and cyclotron frequencies is a turn-by-turn cumulative effect and sets a limit to the highest velocity, $\beta = \mathrm{v/c} \approx 0.22$, $\Delta \mathrm{T}/\mathrm{T_{rev}} \approx 2 - 3\%$. This will be addressed in Sec. 1.2.4. For the time being: this means for instance a limit of applicability of the "classical cyclotron" in the region $\mathrm{E} - \mathrm{mc}^2 \lesssim 25\,\mathrm{MeV}$ for protons, $\lesssim 50\,\mathrm{MeV}$ for D and α particles.

1.2.1 *Fixed-energy orbits, revolution period*

• **Exercise 1.2.1-1.** *Numerical convergence of the integration method: field model and integration step size.*
In view of the exercises in the next sections, we will work from now on with a 60^o sector dipole (thus 6 setors are needed to model the cyclotron).
a - Compute the field map of a 60^o sector, with the same mesh density as used in Ex. 1.1: radial increment of the mesh $\Delta R = 0.5\,\mathrm{cm}$, axial increment $\Delta\theta = 0.5\,\mathrm{cm/RM}$ (the fortran program in App. 1.5.1 can be used again).
- Check the evolution of the cyclotron orbit radius and revolution period with field map mesh density, namely, compute a second field map with increments ΔR and $\Delta\theta$ twice as large; plot the orbit radius R and revolution time $\mathrm{T_{rev}}$ as a function of the kinetic energy $\mathrm{E_k}$ (say, $\mathrm{E_k} : 1 \to 5\,\mathrm{MeV}$) in both cases. Repeat with additional field maps with decreasing mesh density, until noticeable changes to these curves are observed. Add on the graph the theoretical curves for R and $\mathrm{T_{rev}}$. Note: a possibility for better assessing the effect of changing the mesh density is, instead, plotting the relative difference $\delta\mathrm{R}/\mathrm{R}$ and $\delta\mathrm{T_{rev}}/\mathrm{T_{rev}}$.
- With the denser mesh map (more accurate field modeling) check the effect of the integration step size on these quantities: plot the orbit radius R and revolution time $\mathrm{T_{rev}}$ (or the relative difference $\delta\mathrm{R}/\mathrm{R}$ and $\delta\mathrm{T_{rev}}/\mathrm{T_{rev}}$) as a function of the kinetic energ $\mathrm{E_k}$, for a few step size values ranging in $1\,\mathrm{mm} - 2\,\mathrm{cm}$, all on the same graph.

b - Use instead Zgoubi's `DIPOLE` analytical modeling for the field over a 60^o sector: no more field map here, the field at the location of the particle is computed from an analytical model, at each integration step. Re-do the step-size test above. Note : The optical sequence for this exercise is given in appendix 1.5.2.
c - From the two series of results, comment on various pros and cons of the two methods, analytical field models and field maps. •

Periodic motion - Horizontal motion in a uniform field cyclotron has no privileged reference orbit: for a given momentum, the initial radius and velocity vector define a particular closed, circular orbit. A particle launched with an axial velocity component on the other hand, drifts vertically linearly with time, as there is no axial restoring force (the field is normal to the horizontal plane). The next Section will investigate the necessary field property, absent in our simplified field model so far, proper to ensure confinement of the multiturn periodic motion in the vicinity of the median plane of the cyclotron dipole magnet.

• Exercise 1.2.1-2. *Observe the two statements above.*
a - First statement: plot trajectories of particles launched with different initial velocity vector (and zero axial velocity component) over one turn. Give their theoretical parametric equation in a Cartesian frame (O;X,Y) centered at the center O of the cyclotron; superimpose with numerical trajectories (the option `IL=2` in `TOSCA` can be used to store particle coordinates through the field maps, step-by-step).
b - Second statement: plot the axial motion of a particle launched with a non-zero initial axial velocity component. Give its theoretical vertical position Z(s) (Z is along the Lab. vertical axis, s is the path length); superimpose with the numerically computed trajectory. •

• Exercise 1.2.1-3. *Unstable motion in uniform field.*
a - Plot two particle trajectories that demonstrate the value of the radial wave number in a uniform field. Conclude on the orbit and on horizontal motion stability.
b - Derive the horizontal and axial transport matrices from raytracing (use `MATRIX[IFOC=11]`, placed in sequence with the optical sequence). Conclude on the stability of charged particle motion in a uniform field. •

1.2.2 *Weak focusing*

In the following, $B_R(R)$, $B_y(R)$ are respectively the radial and axial components of the magnetic field at R. Median-plane symmetry of the field is assumed, so that $B_R|_{y=0} = 0$ at all R (Fig. 1.10-right).

• Exercise. Show that the mid-plane symmetry hypothesis results in $B_R|_{y=0} = 0$. •

Introduce the small radial distance

$$x(s) = R(s) - R_0 \ll R_0 \tag{1.4}$$

from a reference radius R_0 (with center the center of the axially symmetric cyclotron magnet, Fig. 1.10). The radial and axial forces experienced by a particle at x write,

to the first order in the radial and axial coordinates, respectively x and y,

$$F_x = m\ddot{x} = -qvB_y(R) + m\frac{v^2}{R_0+x} \approx -qv(B_y(R_0) + \left.\frac{\partial B_y}{\partial R}\right|_{R_0} x) + m\frac{v^2}{R_0}(1-\frac{x}{R_0})$$
$$F_y = m\ddot{y} = qvB_R(R) = qv\left.\frac{\partial B_R}{\partial y}\right|_{y=0} y + \text{higher order} \approx qv\frac{\partial B_y}{\partial R}y \qquad (1.5)$$

Note the following two steps in deriving these expressions:

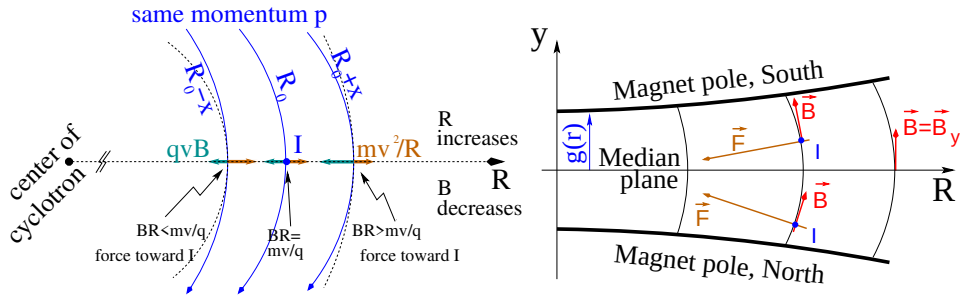

Fig. 1.10 Motion stability in a weak focusing axially symmetric structure. Left, radial: the resultant of the bending and outward forces pulls particles with momentum p = mv toward the equilibrium orbit at $R_0 = p/qB_0$, resulting in a stable oscillation around the latter. Right, axial: positive ions off the median plane (at I, coming out of the page) experience a force pulling toward the median plane.

- the force F_x which applies on the ion is the resultant of the pseudo force $f_c = m\frac{v^2}{R}$, oriented away from the center of the motion, and of the magnetic force $f_B = -qvB_y(R)$, oriented toward the center of the motion. In particular, $-qvB_y(R_0) + m\frac{v^2}{R_0} = 0$.
- a Taylor expansion of the magnetic field yields a first order expression of the r-dependence,

$$B_y(R_0+x) = B_y(R_0) + x\left.\frac{\partial B_y}{\partial R}\right|_{R_0} + \frac{x^2}{2!}\left.\frac{\partial^2 B_y}{\partial R^2}\right|_{R_0} + ... \approx B_y(R_0) + x\left.\frac{\partial B_y}{\partial R}\right|_{R_0}$$

The relations Eq. 1.5 yield the differential equations for the radial and axial motions, respectively,

$$\ddot{x} + \omega_r^2 x = 0 \qquad \text{and} \qquad \ddot{y} + \omega_y^2 y = 0 \qquad (1.6)$$

wherein

$$\omega_r^2 = \omega_{rev}^2(1 + \frac{R_0}{B_0}\frac{\partial B_y}{\partial R}), \quad \omega_y^2 = -\omega_{rev}^2\frac{R_0}{B_0}\frac{\partial B_y}{\partial R} \qquad (1.7)$$

noting $B_y(R_0) = B_0$, and with $\omega_{rev} = 2\pi f_{rev}$ the angular frequency of the circular motion. Focusing by a restoring force appears (Eq. 1.6) owing to the use of a magnetic field with radial index

$$k = \frac{R_0}{B_0}\frac{\partial B_y}{\partial R}|_{R=R_0,y=0} \qquad (1.8)$$

Radial stability in an axially symmetric structure with weakly decreasing field B(R) is sketched in Fig. 1.10-left : At larger motion radius, $R > R_0$ (resp. smaller,

$R < R_0$), a particle with momentum $p = mv$ (assumed positively charged) experiences a decrease (resp. increase) of the outward force $f_c = m\frac{v^2}{R}$ at a higher rate than the decrease (resp. increase) of the bending force $f_B = -qvB$. In other words, radial stability requires BR to be an increasing function of R, $\frac{\partial BR}{\partial R} = B + R\frac{\partial B}{\partial R} > 0$, this holds in particular at R_0 thus $1 + k > 0$.

Axial stability imposes a guiding field decreasing with radius, Fig. 1.10-right, *i.e.*, $k < 0$, this ensures a restoring force directed toward the median plane.

The resulting condition of motion stability around the equilibrium orbit

$$-1 < k < 0 \tag{1.9}$$

The two quantities in Eq. 1.7

$$\nu_R = \omega_r/\omega_{rev} = \sqrt{1+k}, \quad \nu_y = \omega_y/\omega_{rev} = \sqrt{-k} \tag{1.10}$$

are known as, respectively, the radial and axial "wave number" (or "tunes"), the number of oscillations of the particle about the reference circular orbit of radius R_0. Note that $\nu_R^2 + \nu_y^2$ takes it value on the unit radius circle in the wave number diagram (ν_R, ν_y).

• **Exercise 1.2.2-1.** *Introducing a radial field index.*
Constant field-gradient focusing ($k \propto \partial B/\partial R$=constant over the beam spiral span) can be obtained from a decrease of the magnetic field proportional to the radius (this can be realized practically by "gap shaping" of the field, a gap slowly opening up, linearly with increasing radius).
a - Use `TOSCA` and the 60^o sector field map of exercise 1.2.1-1, construct the sector field map accounting for a radial index k: take the 200 keV injection radius R_0 as the reference radius in this exercise (R_0 is required to define the index k, Eq. 1.8). Track that 200 keV orbit, plot it in the lab frame: make sure it comes out as expected, namely, closed and periodic: final and initial position and angle equal.
b - Find the orbit radius R(p) numerically, for a series of rigidity values such to cover the extent of the field map (use the `FIT` procedure to find R for a given particle rigidity and `REBELOTE` to repeat); plot both numerical and theoretical $B\rho(R)$ (use `FAISTORE` storage command placed between `FIT` and `REBELOTE`).
c - Plot the axial paraxial motion of a 1 MeV proton, over a few turns (use as earlier, `IL=2` under `TOSCA` and the data so logged to zgoubi.plt). Check the effect of the focusing strength by comparing the trajectories for a few different index values, including close to -1 or close to 0.
d - Plot the magnetic field experienced by the particle along these trajectories. •

• Exercise 1.2.2-2. *A radial field index in `DIPOLE`.*
Introduce a radial field index, using the analytical modeling `DIPOLE`. A template input file to Zgoubi is guven in App. 1.5.2.
Repeat questions a to d of exercise 1.2.2-1. •

Isochronism - The focusing condition $-1 < k < 0$ breaks the isochronism as it causes the guiding field B and thus $\omega_{rev} = qB/m$ to change (decrease) with R. As a consequence, the arrival time of a particle at the RF gap (by extension the "RF phase" of the motion) is not constant (this is addressed in Sec. 1.2.4).

1.2.3 *Coordinate transport*

Introducing the path variable, s, as the independent variable in Eq. 1.6 and using the approximation $ds \approx v dt$, Eqs. 1.6 take the form

$$\frac{d^2x}{ds^2} + \frac{1+k}{R_0^2}x = 0, \qquad \frac{d^2y}{ds^2} + \frac{-k}{R_0^2}y = 0 \tag{1.11}$$

The solutions write, for respectively the horizontal and vertical motions,

$$\begin{cases} R(s) - R_0 = x(s) = x_0 \cos\frac{\sqrt{1+k}}{R_0}(s-s_0) + x'_0 \frac{R_0}{\sqrt{1+k}} \sin\frac{\sqrt{1+k}}{R_0}(s-s_0) \\ R'(s) = x'(s) = \quad -x_0 \frac{\sqrt{1+k}}{R_0} \sin\frac{\sqrt{1+k}}{R_0}(s-s_0) + x'_0 \cos\frac{\sqrt{1+k}}{R_0}(s-s_0) \end{cases} \tag{1.12}$$

$$\begin{cases} y(s) = \ y_0 \cos\frac{\sqrt{-k}}{R_0}(s-s_0) + y'_0 \frac{R_0}{\sqrt{-k}} \sin\frac{\sqrt{-k}}{R_0}(s-s_0) \\ y'(s) = -y_0 \frac{\sqrt{-k}}{R_0} \sin\frac{\sqrt{-k}}{R_0}(s-s_0) + y'_0 \cos\frac{\sqrt{-k}}{R_0}(s-s_0) \end{cases} \tag{1.13}$$

• Exercise 1.2.3-1. *Projected particle trajectories.*
Plot the horizontal and vertical trajectories x(s) and y(s) of a particle, over 2-3 turns in the cyclotron. Plot the difference with numerical values from Eq. 1.13, verify that raytracing outcomes satisfy the theory (use the option `IL=2` to store particle coordinates in zgoubi.plt, step-by-step). •

Note that the dissymmetry between the conditions of horizontal stability (term "1" in "$\sqrt{1+k}$") and vertical stability ("$\sqrt{-k}$" instead) arises from the focusing introduced by the curvature, a purely geometrical effect. The focal distance associated with the curvature of a magnet of arc length $\mathcal{L}$ is obtained by integrating $\frac{d^2x}{ds^2} + \frac{1}{R_0^2}x = 0$ and identifying with the focusing property $\Delta x' = -x/f$, namely,

$$\Delta x' = \int \frac{d^2x}{ds^2} ds \approx \frac{-x}{R^2} \int ds = \frac{-x\mathcal{L}}{R^2}, \quad \text{thus} \quad f = \frac{R^2}{\mathcal{L}}$$

• Exercise 1.2.3-2. *Transverse phase space, phase space motion.*
Track a particle with small amplitude radial and axial motions, at constant energy, in a ring cyclotron based on the earlier material.
a - Plot $x(s) - R_0$ (or y(s)) around the ring over 3-4 turns. Check that the observed fraction of wavelength per turn (radial or axial), identifies with the wave number (hint: use a fitting procedure to match the trajectory with the expected Eq. 1.12 - or Eq. 1.13 in the case of y(s) motion).
b - Record particle coordinates x, y at some fixed azimuth s around the ring, compute its radial and axial wave numbers by Fourier analysis. What is the indetermination on the wave number? Explain.
c - At some azimuth s around the ring, observe the coordinates (x,x') of a particle as it circles around, plot them in the "transverse phase-space", (x,x'). Using the trajectory Eq. 1.12 show that the particle trajectory in phase space is on an ellipse. Superimpose that ellipse on the particle moti in the previous graph.

Chromatism, chromatic orbit - In an axially symmetric structure, the equilibrium trajectory at momentum $\begin{cases} p_0 \\ p_A \end{cases}$ is at radius $\begin{cases} R_0 \text{ such that } B_0R_0 = p_0/q \\ R_A \text{ such that } B_AR_A = p_A/q \end{cases}$, with $\begin{cases} B_A = B_0 + \left(\frac{\partial B}{\partial x}\right)_0 + ... \\ R_A = R_0 + \Delta x \\ p_A = p_0 + \Delta p, \end{cases}$
On the other hand

$$B_AR_A = \frac{p_A}{q} \Rightarrow \left[B_0 + \left(\frac{\partial B}{\partial x}\right)_0 \Delta x + ...\right][R_0 + \Delta x] = \frac{p_0 + \Delta p}{q} = \frac{p_0}{q} + \frac{\Delta p}{q}$$

and, neglecting terms in $(\Delta x)^2$: $B_0R_0 + \left(\frac{\partial B}{\partial x}\right)_0 R_0\Delta x + B_0\Delta x = \frac{p_0}{q} + \frac{\Delta p}{q}$, which, given $B_0R_0 = \frac{p_0}{q}$, leaves $\Delta x\left[\left(\frac{\partial B}{\partial x}\right)_0 R_0 + B_0\right] = \frac{\Delta p}{q}$, which given $n = -\frac{R_0}{B_0}\left(\frac{\partial B}{\partial x}\right)_0$ yields

$$\Delta x = \frac{R_0}{1+k}\frac{\Delta p}{p_0} = D\frac{\Delta p}{p_0} \tag{1.14}$$

In passing we have introduced the quantity $D = \frac{R_0}{1+k}$, the "dispersion" factor with

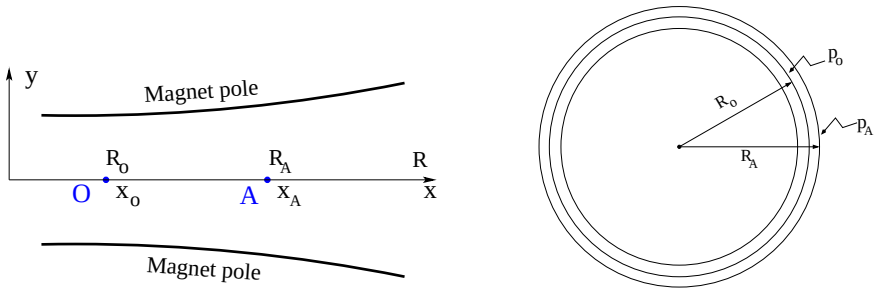

Fig. 1.11 The equilibrium radius at location $O(x = x_0)$ is $R = R_0$, the equilibrium momentum is p_0, rigidity $BR = B_0R_0$. The equilibrium radius at $A(x = x_A)$ is $R = R_A$ for the particle with momentum $p_A = p_0 + \Delta p$, rigidity $BR = B_AR_A$.

respect to the reference closed orbit at R_0. This establishes that, when R_0 or k are s-dependent quantities (as in the synchrotron, next Chapters), D(s) is the solution of the differential equation

$$\frac{d^2D(s)}{ds^2} + \frac{1+k}{R_0^2}D(s) = \frac{1}{R_0} \tag{1.15}$$

However D is a constant in the present case of the non-relativistic cyclotron (k is constant by definition, and $R_0 = p_0/qB_0$ is constant).

1.2.4 *Resonant acceleration*

An oscillating radio-frequency (RF) electric field, with fixed-frequency f_{rf} is applied in the gap between the two dees (Fig. 1.5). An ion of charge q reaching the gap at time t undergoes a change in energy

$$\Delta W(t) = q\hat{V}\sin\phi \quad \text{with } \phi = \omega_{rf}t - (\omega_{rev}t + \phi_0) \tag{1.16}$$

with ϕ the RF phase experienced by the particle at the time it crosses the gap and ϕ_0 the origin in phase for the particle motion (normally about $\pi/2$, in the region of the crest of V(t) oscillation). Note that this ignores the "transit time", the effect of the time that the particle spends across the gap on the overall energy gain; focusing in the cyclotron, in what follows, will ignore as well the effect of the electric gap.

The frequency dependence of the kinetic energy W of the ion relates to its orbital radius R in the following way:

$$W = \frac{1}{2}mv^2 = \frac{1}{2}m(2\pi R f_{rev})^2 \approx \frac{1}{2}m(2\pi R\frac{f_{rf}}{h})^2 \tag{1.17}$$

thus, for a given cyclotron size (R), f_{rf} and h set the limit for the acceleration range.

The revolution time/frequency increases/decreases with energy and the condition of synchronism with the oscillating voltage, $f_{rf} = hf_{rev}$, is only fulfilled at one particular radius in the course of acceleration (Fig. 1.12). To the left and to the right, out-phasing $\Delta\phi$ builds-up turn after turn, decreasing in a first stage (towards zero, $\phi < \pi/2$ and lower voltages, Fig. 1.12-right) and then increasing back to $\phi = \pi/2$ phase and beyond towards $\phi = \pi$ - the boundary for the acceleration mode.

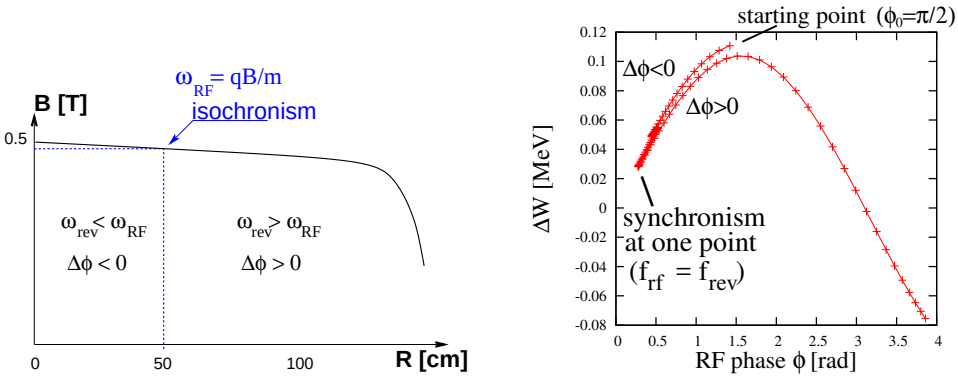

Fig. 1.12 Synchronous condition at one point (left), h=1 assumed here, and span in phase of the energy gain $\Delta W = q\hat{V}\sin\phi$ over the acceleration cycle (right). ϕ is the phase of the RF sine wave at arrival of the particle at the accelerating gap. Note that the vertical separation of the two $\Delta W(\phi)$ branches on the right ($\Delta\phi < 0$ and $\Delta\phi > 0$) is artificial, this is for clarity, they are actually superimposed.

Differentiating the particle phase at the RF gap, over a half-turn (Eq. 1.16 with ω_{rev} constant between two gaps) one gets $\dot{\phi} = \omega_{rf} - \omega_{rev}$. Over a half-turn in addition, $\Delta\phi = \dot{\phi}\frac{\pi R}{v}$, yielding a phase-shift per half-turn of

$$\Delta\phi = \pi\left(\frac{m\omega_{rf}}{qB} - 1\right) \tag{1.18}$$

Due to this cumulative out-phasing the classical cyclotron requires quick acceleration (limited number of turns), which means high voltage (tens or hundreds of kVolts). As expected, with ω_{rf} and B constant, $\Delta\phi$ presents a minimum ($\dot{\phi} = 0$) at $\omega_{rf} = \omega_{rev} = \frac{qB}{m}$ where exact isochronism is reached (Fig. 1.12). The upper limit to ϕ is set by the condition $\Delta W > 0$, acceleration.

• Exercise 1.2.4-1. *RF phase shift at the accelerating gap.*
Consider the cyclotron model of exercise 1.2.2-2 (which uses `DIPOLE` and a double accelerating gap). Take the following parameters: field index k = −0.03125, field $B_0 = 5\,kG$ on injection radius, injection energy $W_0 = 200\,keV$, peak gap voltage $\hat{V} = 100\,kV$. Assume, first, that the acceleration is independent of the arrival phase (use `CAVITE[IOPT=3]`, at both gaps).
a - Track a proton from 1 to 5 MeV: get the turn-by-turn phase-shift at the gap, compare with Eq. 1.18.
b - Produce a similar diagram $\Delta W(\phi)$ to Fig. 1.12-right. •

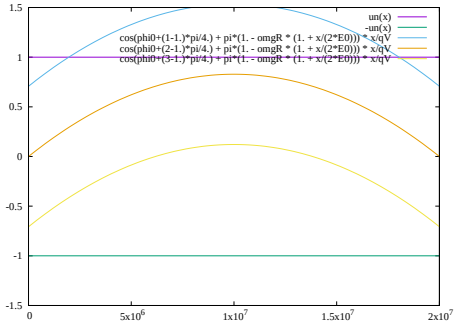

Fig. 1.13 The cyclotron equation.

• Exercise 1.2.4-2. *The cyclotron equation*
relates RF phase ϕ and particle energy E, it writes [6]

$$\cos\phi = \cos\phi_i + \pi\left[1 - \frac{\omega_{rf}}{\omega_{rev}}\frac{E + E_i}{2E_0}\right]\frac{E - E_i}{q\hat{V}} \tag{1.19}$$

(E=W+E_0 =total energy, E_0 =rest mass, index i denotes injection) and is represented in Fig. 1.13 for various values of RF phase at injection ϕ_i. The cyclotron model of exercise 1.2.4-1 may be used here.
a - In an attempt to accelerate over a kinetic energy range of about $[0.2, 20]$ MeV, assume maximum of $\cos(\phi)$ at $W_m = 10\,MeV$. From $d(\cos\phi)/dW = 0$ at W_m, deduce the operation RF frequency (assume RF harmonic h=1).
Set up the Zgoubi model accordingly. **b -** Plot the theoretical energy-phase relationship characteristic of the cyclotron acceleration: for $\phi_0 = \frac{3\pi}{4}, \frac{\pi}{2}, \frac{\pi}{4}$, from both simulation and theory •

1.3 Relativistic cyclotron

The bad news with relativistic effects is that the particle slows down with energy and loses synchronism. From the cyclotron resonance $\omega_0 = qB/\gamma m_0$, given $R = \beta c/\omega_0$, one gets the particular relationship

$$k = \frac{R}{B}\frac{\partial B}{\partial R} = \frac{\beta}{\gamma}\frac{\partial\gamma}{\partial\beta} = \beta^2\gamma^2 \tag{1.20}$$

Thus synchronism requires $\frac{R}{B}\frac{\partial B}{\partial R} = k$ to be positive and increasing with energy: the weak focussing condition $-1 < k < 0$ is not satisfied, transverse stability is lost.

Note also that, by constrast to the earlier weak-focusing conditions, k can no longer be a constant, it has to increase with R. Thus the wave numbers (Eq. 1.10) also change with R (in particular, the horizontal wave number follows γ, a consequence of the isochronism, this will be discussed later).

• Exercise 1.3-1. In passing, demonstrate the following relationships: $\frac{dp}{p} = \frac{1}{\beta^2}\frac{dE}{E}$; $\frac{d\beta}{\beta} = \frac{1}{\gamma^2}\frac{dp}{p} = \frac{1}{\beta^2\gamma^2}\frac{dE}{E}$; $\frac{d\gamma}{\gamma} = \frac{dW}{m_0+W}$ (W = kinetic energy); $\frac{dW}{W} = \frac{\gamma+1}{\gamma}\frac{dp}{p}$. •

The revolution period on the equilibrium orbit, momentum $p = qBR$ and circumference $\mathcal{C}$, is $T = \mathcal{C}/\beta c = 2\pi\gamma m_0/qB$. Isochronism requires p-invariant revolution period, $dT/dp = 0$. Differentiating the previous expression, this requirement yields

$$B(R) = \frac{B_0}{\gamma_0}\gamma(R) \tag{1.21}$$

with B_0 and γ_0 free reference conditions, and the reference revolution period is noted T_0. In other words, isochronism requires $B(R) \propto \gamma$, and this yields axial defocusing.

H.A. Bethe and M.E. Rose once stressed [3] "... it seems useless to build cyclotrons of larger proportions than the existing ones... an accelerating chamber of 37 cm radius will suffice to produce deuterons of 11 MeV energy which is the highest possible...". Frank Cole : "If you went to graduate school in the 1940s, this inequality $[-1 < k < 0]$ was the end of the discussion of accelerator theory."

Until...

1.3.1 *Thomas focusing*

In 1938, L.H. Thomas introduces the concept of alternating regions of stronger and weaker axial field [4], the "AVF" (Azimuthally Varying Field) cyclotron (Fig. 1.14). The single-magnet concept of the classical cyclotron remains, however an azimuthal field modulation is introduced by shaping the magnet pole to create a $2\pi/N$-periodical field modulation. From this results a form factor, the "flutter", for instance of sinusoidal form

$$\mathcal{F}(\theta) \propto 1 + f\sin(N\theta) \tag{1.22}$$

The necessary radial increase of the field for preserving the isochronism of the orbits in the relativistic regime (Eq. 1.21) is obtained by radial pole shaping. The median plane field now varies with both R and θ,

$$B(R,\theta) = B_0\,\mathcal{R}(R)\,\mathcal{F}(\theta) \tag{1.23}$$

Note that the orbit curvature is no longer constant along the orbit (which is no longer a circle) as a consequence of the AVF, for this reason a local curvature radius $\rho(s)$ is introduced in the following, in lieu of the former R assumed up to now constant over the 2π circular orbit. R instead will in general be used to denote the average radius of the closed, periodic orbit, $R = \oint ds/2\pi$.

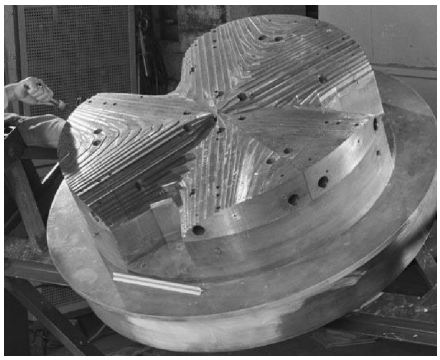

Fig. 1.14 Azimuthal pole shaping in Thomas-style AVF cyclotron.

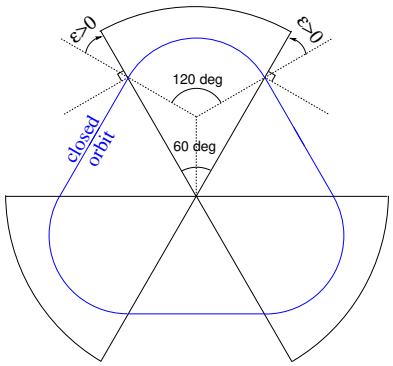

Fig. 1.15 Sketch of a 3-period, 120^o sector, AVF cyclotron. The optical axis (or reference "closed orbit") is at $\epsilon = 30^o$ "wedge angle" with the sector dipole edge. This is a "closing" of the magnet, it causes vertical focusing and weakens the horizontal focusing (*cf.* Fig. 1.17).

A sector dipole with field index

We now introduce the transfer matrix of a sector magnet, pushing Thomas' modulation to the point that the field varies abruptly between 0 and B_0 at sector edges (a simplified, so-called "hard-edge", model of a sector dipole). Bending sections span a fraction of 2π and the "filling factor" (ratio $\mathcal{L}_{\rm mag}/2\pi R$ of the magnetic length to the orbit length) is < 1.

Eqs. 1.12 1.13 which express the transport of the coordinate of a particle as it propagates through the hard-edge bending sector, can be written under matrix form, namely

$$\begin{pmatrix} x \\ x' \\ y \\ y' \end{pmatrix}_{\rm out} = \begin{pmatrix} \cos\sqrt{k_x}\mathcal{L} & \frac{1}{\sqrt{k_x}}\sin\sqrt{k_x}\mathcal{L} & 0 & 0 \\ -\sqrt{k_x}\sin\sqrt{k_x}\mathcal{L} & \cos\sqrt{k_x}\mathcal{L} & 0 & 0 \\ 0 & 0 & \cos\sqrt{k_y}\mathcal{L} & \frac{1}{\sqrt{k_y}}\sin\sqrt{k_y}\mathcal{L} \\ 0 & 0 & -\sqrt{k_y}\sin\sqrt{k_y}\mathcal{L} & \cos\sqrt{k_y}\mathcal{L} \end{pmatrix} \begin{pmatrix} x \\ x' \\ y \\ y' \end{pmatrix}_{\rm in} \tag{1.24}$$

wherein "*in*" and "*out*" stand for the entrance ($s = s_{\rm in}$) and exit ($s = s_{\rm out}$) of the sector, $k_x = (1+k)/\rho^2$, $k_y = n/\rho^2$, $\mathcal{L}$ is the length of the arc of curvature ρ (which coincides with the trajectory of reference momentum $p = mv$ at radius R). The null anti-diagonal coefficients in this 4×4 matrix representation express the fact that the radial and axial components of the motion are independent, "*decoupled*". Thus the transport can be expressed for Eq. 1.12 and Eq. 1.13 independently, under the form of a 2×2 matrix relationship,

$$\begin{pmatrix} x \\ x' \end{pmatrix}_{\rm out} = \begin{pmatrix} \cos\sqrt{k_x}\mathcal{L} & \frac{1}{\sqrt{k_x}}\sin\sqrt{k_x}\mathcal{L} \\ -\sqrt{k_x}\sin\sqrt{k_x}\mathcal{L} & \cos\sqrt{k_x}\mathcal{L} \end{pmatrix} \begin{pmatrix} x \\ x' \end{pmatrix}_{\rm in} \tag{1.25}$$

$$\begin{pmatrix} y \\ y' \end{pmatrix}_{out} = \begin{pmatrix} \cos\sqrt{k_y}\mathcal{L} & \frac{1}{\sqrt{k_y}}\sin\sqrt{k_y}\mathcal{L} \\ -\sqrt{k_y}\sin\sqrt{k_y}\mathcal{L} & \cos\sqrt{k_y}\mathcal{L} \end{pmatrix} \begin{pmatrix} y \\ y' \end{pmatrix}_{in} \tag{1.26}$$

• Exercise 1.3.1-1. *Transport matrix.*
Compute the 4×4 transport matrix of a 60^o sector with index $-1 < k < 0$ (say,

k = −0.6) and curvature ρ for the reference momentum p (as in Fig. 1.16), from the raytracing of an appropriate set of paraxial rays (hint: use `OBJET`, option KOBJ=5, to define the particle set, and `MATRIX` to compute the matrix). Compare with theory. •

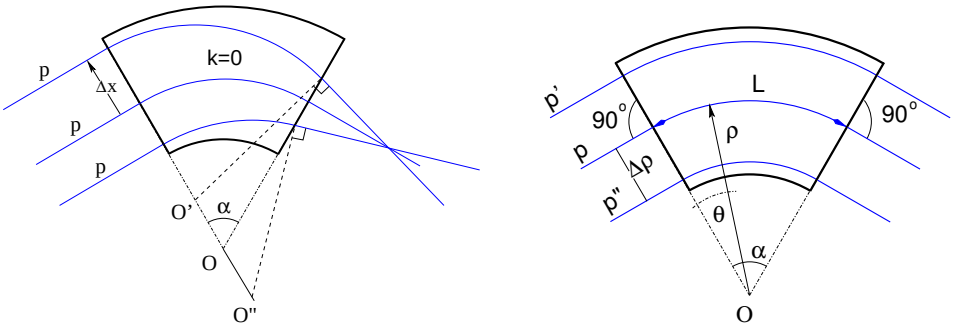

Fig. 1.16 Left: ** REFAIRE** field index k = 0, parallel incoming rays of equal momenta come out converging - radial trajectory convergence (focusing) in a uniform field sector dipole is a purely geometrical property. Right: an $\alpha = 60^o$ sector dipole with index k. At constant radius, B is constant, a particle with *small* momentum deviation $\Delta p = q(1+k)B\Delta\rho$ will follow an arc of radius $\rho + \Delta\rho$.

• Exercise 1.3.1-2. The focal distance associated with the curvature (index k = 0, magnet length $\mathcal{L}$ and curvature radius ρ) satisfies

$$\frac{d^2x}{ds^2} + \frac{1}{\rho^2}x = 0 \Rightarrow \Delta x' = \int \frac{d^2x}{ds^2} ds \approx -\frac{x}{\rho^2}\int ds = -\frac{x}{\rho^2}\mathcal{L} \overset{\text{def.}}{\equiv} -\frac{x}{f} \Rightarrow f = \frac{\rho^2}{\mathcal{L}}$$

Verify the value of f in the case of a $\alpha = 60^o$ sector dipole with index n, by raytracing paraxial rays with incoming incidence zero and coordinates ±x. •

• Exercise 1.3.1-3. *Geometrical focusing in a dipole. Focusing index.*
Geometrical focusing in a constant field dipole stems from the longer (shorter) path in the magnetic field for rays entering the magnet at greater (smaller) radius.
a - Raytrace three rays with identical momentum entering at respectively $R^- < R_0 < R^+$, through a $\alpha = 60^o$ sector dipole with zero field index, as in Fig. 1.16-left. Show that the field integrals through the magnet satisfy $\int B\, ds/B\rho = \theta$, and thus $\theta^- < \theta_0 < \theta^+$.
b - This effect can be cancelled if particles at greater (smaller) radius find a smaller (greater) field: this would result in ΔB such that $\Delta x = OO' = 0$, $\Delta x = O''O = 0$, in Fig. 1.16. Differentiation of $B\rho = C^{st}$ yields $\frac{\Delta B}{B} + \frac{\Delta\rho}{\rho} = 0$, hence a required index $k = \frac{\rho}{B}\frac{\Delta B}{\Delta x} = -1$. Verify that property by raytracing three parallel incoming rays of equal momenta. •

Wedge focusing

Note in passing: wedge focusing would eventually be the technique used for the ZGS, "Zero Gradient Synchrotron", a 12 GeV ring at Argonne. This will be addressed in

the weak focusing synchrotron chapter. The interest is that it simplifies the sector magnet as it avoids profiling its poles (as the transverse field index is null).

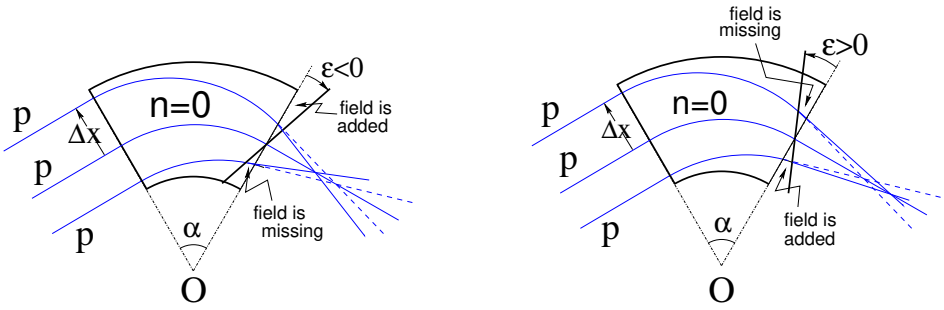

Fig. 1.17 Left: a focusing wedge ($\epsilon < 0$ by convention), opening the sector augments the horizontal focusing. Right: a defocusing wedge ($\epsilon > 0$ by convention), closing the sector diminishes the horizontal focusing. Focal distance in the bend plane respectively decreases, increases. The reverse holds in the vertical plane, opening/closing the sector decreases/increases the vertical focusing.

The transport of the transverse (radial and axial) particle coordinates through a dipole magnet edge, with wedge angle ϵ can be written under the matrix form

$$\begin{pmatrix} x \\ x' \\ y \\ y' \end{pmatrix}_2 \begin{pmatrix} 1 & 0 & 0 & 0 \\ -\tan\frac{\epsilon}{\rho} & 1 & 0 & 0 \\ 0 & 0 & 1 & 0 \\ 0 & 0 & \tan\frac{\epsilon}{\rho} & 1 \end{pmatrix} \begin{pmatrix} x \\ x' \\ y \\ y' \end{pmatrix}_1 \tag{1.27}$$

The transport matrix of a dipole magnet with wedge angles ($\epsilon \neq 0$) writes

$$\mathrm{M} = \mathrm{W_o} \times \mathrm{M_{sector}} \times \mathrm{W_i} \tag{1.28}$$

with $\mathrm{W_o}$, exit wedge (respectively $\mathrm{W_i}$, entrance wedge) a matrix of the form Eq. 1.27 and $\mathrm{M_{sector}}$ as in Eq. 1.24.

• Exercise 1.3.1-4. From raytracing, get the transport matrix of a 120° sector in the two cases of (i) no wedge angle, (ii) 30° wedge angle at entrance and exit as sketched in Fig. 1.15. Show that in the second case the dipole is both radially and axially focusing. Check against Eq. 1.27 . •

• Exercise 1.3.1-5. *Wave numbers from the transport matrix.*
a - Compute the R-dependence of the radial and axial wave numbers ν_R and ν_y of the circular motion, using 1-turn mapping (use `MATRIX` to get the wave numbers, `FIT` to get the closed orbit for a particular momentum, and `REBELOTE` to scan a momentum range).
b - Show that, for all R, $\nu_\mathrm{R}^2 + \nu_\mathrm{y}^2 = 1$. •

The "flutter" F characterizes the steepness of the azimuthal field fall-off $\mathcal{F}(\theta)$ (*e.g.*, as in Eq. 1.22) over an extent λ at magnet ends. For a given orbit, of average radius

$\mathrm{R} = \oint \mathrm{ds}/2\pi$ and of curvature $\rho(\mathrm{s})$ inside the dipole, it writes

$$\mathrm{F} = \left(\frac{< \mathcal{F}^2 > - < \mathcal{F} >^2}{< \mathcal{F} >^2} \right)^{1/2} \quad \stackrel{\lambda \to 0}{\longrightarrow} \quad \frac{\mathrm{R}}{\rho} - 1 \tag{1.29}$$

with $\mathrm{F} = \frac{\mathrm{R}}{\rho} - 1$ the "hard-edge" field fall-off case, *i.e.*, the (unphysical) case when $\mathcal{F}(\theta)$ steps from 1 to 0 at the location of the magnet edge. Edge focussing makes possible the necessary $\mathrm{B(R)} \propto \gamma(\mathrm{R})$ (Eq. 1.21) as it ensures the axial focusing which would otherwise be lost due to $\mathrm{k} > 1$. If the scalloping of the orbit is small, *i.e.*, if $\mathcal{C}/2\pi \approx \rho$ (*i.e.*, the presence of drifts only causes a small departure of the $\mathcal{C}$-circumference closed orbit from the average radius $\mathcal{C}/2\pi$), then

$$\nu_\mathrm{x} \approx \sqrt{1 + \mathrm{k}} \ \text{ and } \ \nu_\mathrm{y} \approx \sqrt{-\mathrm{k} + \mathrm{F}^2} \tag{1.30}$$

in a first approach. The flutter causes $\mathrm{n} + \mathrm{F}^2 > 0$ (whereas $\mathrm{n} < 0$, B increases with R for isochronism) thus the vertical motion is stable in the sense of periodic stability (ν_y is real). Expectedly from what precedes, the fringe field modifies the first order vertical mapping, namely, the vertical wedge focussing (Eq. 1.27) is changed in the following way:

$$\mathrm{R}_{43=} \frac{\tan(\epsilon)}{\rho} \to \mathrm{R}_{43} = \frac{\tan(\epsilon - \psi)}{\rho} \tag{1.31}$$

wherein

$$\psi = \mathrm{I}_1 \frac{\lambda}{\rho} \frac{1 + \sin^2 \epsilon}{\cos \epsilon}, \quad \text{with } \mathrm{I}_1 = \int_{\mathrm{s(B=0)}}^{\mathrm{s(B=\overline{B})}} \frac{\mathrm{B(s)(B_0 - B(s))}}{\mathrm{B}_0^2} \frac{\mathrm{ds}}{\lambda} \tag{1.32}$$

and the integral I_1 extends over the field fall-off where B evolves between 0 to some plateau value $\overline{\mathrm{B}}$ inside the magnet. To the first order the horizontal focusing is not affected by the fall-off extent λ, the first order mapping of Eq. 1.27 is unchanged.

• Exercise 1.3.1-5. *Fringe field extent and wedge focusing.*
Play with the extent λ of the fringe field in the 120^o sector dipole of Ex. 1.3.1-5: from extremely short (quasi hard-edge) to very long. Check the evolution of horizontal and vertical focusing of the magnet, and of the wave numbers of the ring. Note: the integration step size in `DIPOLE` has to be made consistent with the value of λ, for the numerical integration to converge properly. •

1.3.2 *Spiral sector*

In 1954 Kerst introduces a method for vertical wedge focusing which compensates for the radially increasing field gradient: by spiraling the edges of the sector dipoles (Fig. 1.3)

$$\mathrm{B}(\mathrm{R}, \theta) = \mathrm{B}_0 \, \mathcal{F}(\mathrm{R}, \theta) \, \mathcal{R}(\mathrm{R}), \quad \mathcal{F}(\mathrm{R}, \theta) = 1 + \mathrm{f} \sin(\mathrm{N}(\theta - \tan(\xi) \ln(\mathrm{R}/\mathrm{R}_0))) \tag{1.33}$$

$R = R_0 \exp(\theta / \tan(\xi))$ is the equation of the spiral, centered at the center of the ring. This results in a larger contribution of the flutter term in the vertical wave number,

$$\nu_\mathrm{y} = \sqrt{-\mathrm{k} + \mathrm{F}^2 (1 + 2 \tan^2 \xi)} \tag{1.34}$$

with ξ the spiral angle: the angle that the tangent to the spiral edge does with the ring radius.

In the late 1950s appeared the "separated sector cyclotron", in which the sector dipoles are separated by iron-free spaces (not really field-free, though, due the the field fall-offs) (Fig. 1.2). Isochronous cyclotrons nowadays still rely on these various principles and techniques, their limit in energy resides in achievable field strength, magnet size, and beam separation at the last turn for extraction.

An instance of a single-magnet spiral sector AVF cyclotron is PSI's 250 MeV protontherapy machine, Fig. 1.3, the field at the center of the cyclotron is 2.4 T. An instance of a separated spiral sector cyclotron is PSI's 590 MeV, Fig. 1.2.

Simulations regarding spiral sector optics will be performed in the FFAG chapter.

1.3.3 *Isochronous acceleration*

Simualtions using a model of the PSI cyclotron (Fig. 1.2) are provided in a separate document, to be found in the CASE web site.

1.3.4 *Cyclotron extraction*

• **Exercise 1.3.4.** *Limit in energy.*
It follows from qBR = p that $\frac{\Delta R}{R} = \frac{***}{***}$. With $***$ the energy gain per turn this yields $\Delta R = \frac{m\Delta E_k}{q^2B^2R}$: the radius increment ΔR decreases with R. As the extraction at the last turn requires sufficient separation from the last but one turn, for insertion of a deflector electrode (see Fig. 1.5), there is a practical feasibility limit. Plot the accelerated spiral, or the fixed-energy orbits, to top energy, observe this property. Plot dR(R), from both tracking and theory. •

1.4 summary

In this Chapter the following has been addressed:

- the uniform field (single-magnet) classical cyclotron, field characterized by $B(\theta)$ =constant,

- weak transverse focusing, in both planes simultaneously, obtained by a slow radial decrease of the field, $B(R) = B_0 + k\frac{B_0}{R_0}(R - R_0)$, $-1 < k < 0$,

- near-crest, quasi-isochronous, resonant acceleration in the classical cyclotron, its limit in energy,

- Thomas "AVF" isochronus cyclotron; azimuthal field modulation ("flutter") and vertical focusing, with for instance $B(\theta) \propto B_0(1 + f\sin(3\theta))$,

- wedge focusing, enhanced vertical focusing by spiraling the pole edges,

- the isochronous cyclotron, a separated sector ring accelerator,

- relativistic resonant acceleration in an isochronous cyclotron.

Various notions and quantities which characterize charged particle dynamics in accelerators have been introduced, including:

- closed orbit,
- focusing and field index,
- differential equations of the motion, and their periodic solutions,
- wave numbers, motion invariant,
- dispersion function,
- transport of particle coordinates,
- transport matrix formalism.

1.5 Appendix

1.5.1 *Field map and optical sequence for Exercise 1.1-1*

The cyclotron is defined using a 180^o field map twice. This optical sequence can be copy-pasted to a Zgoubi input data file and run as it is, once the magnetic field map has been built (and saved in "geneSectorMap.out").

Consult zgoubi users' guide for the functionning of the various keywords (`OBJET`, `PARTICUL`, `FAISTORE`, `TOSCA`, `FAISCEAU`, `END`) and their subsequent data list.

Fortran program that generates a field map

This program builds a 180^o magnetic field map in the appropriate format for zgoubi's `TOSCA [IX=315,IY=121,IZ=1,MOD=22]` field map reading mode. Save it in "geneSectorMap_180deg.out" for this exercise.

```
      implicit double precision (a-h,o-z)
      parameter (pi = 4.d0*atan(1.d0))

C------------ Hypothesis :
C Total angle extent of the field map. Can be changed, e.g., to 360, 0r 60 deg, or else.
C      AT = 360.d0  /180.d0*pi
       AT = 180.d0  /180.d0*pi
C Take RM=50 cm reference radius, as this (arbitray) value is found in other exercises
       RM = 50.d0
C dR is the radial distance between two nodes, good starting point is dR = 0.5 cm
       dR = 0.5d0            ! cm, mesh step in radius, approximate: allows getting NR
C dX=RM*dA is the arc length between two nodes along R=RM arc, given angle increment dA
C A good starting point (by experience) is dX a few mm, say ~0.5 cm
       dX = 0.5d0             ! cm, mesh step at RM, approximate: allows getting NX

C------------ Outcomes :
C Radial extent of the field map
       Rmi = 1.d0   ! cm
       Rma = 76.d0   ! cm
       NR = NINT((Rma - Rmi) / dR) +1
       dR = (Rma - Rmi) / dble(NR -1)   ! make sure (NR-1)*dR == Rma-Rmi
C dX=RM*dA is the arc length between two nodes along R=RM arc, given angle increment dA
       NX = NINT(RM*AT / dX)  +1
       dX = RM*AT / DBLE(NX - 1)  ! exact mesh step at RM, corresponding to NX
       dA = dX / RM               ! corresponding delta_angle
       A1 = 0.d0 ; A2 = AT
C-----------------------------------------------

       BY = 0.d0 ; BX = 0.d0 ; Z = 0.d0
       BZ = 5.d0  ! kG

       open(unit=2,file='geneSectorMap.out')
       write(2,*) Rmi,dR,dA/pi*180.d0,dZ,
      >'     !  Rmi/cm, dR/cm, dA/deg, dZ/cm'
       write(2,*) '# Field map generated using geneSectorMap.f '
       write(2,fmt='(a)') '# AT/rd,  AT/deg, Rmi/cm, Rma/cm, RM/cm,'
      >//' NR, dR/cm, NX, dX/cm, dA/rd : '
       write(2,fmt='(a,1p,5(e16.8,1x),2(i3,1x,e16.8,1x),e16.8)')
      >'# ',AT, AT/pi*180.d0,Rmi, Rma, RM, NR, dR, NX, dX, dA
       write(2,*) '# For TOSCA: ',NX,NR,' 1 22.1 1.  !IZ=1 -> 2D ; '
      >//'MOD=22 -> polar map ; .MOD2=.1 -> one map file'
       write(2,*) '# R*cosA (A:0->360), Z==0, R*sinA, BY, BZ, BX '
       write(2,*) '# cm                 cm    cm      kG  kG  kG '
       write(2,*) '# '

       do jr = 1, NR
         R = Rmi + dble(jr-1)*dR
         do ix = 1, NX
           A = A1 + dble(ix-1)*dA
C           write(2,fmt='(1p,6(e16.8),a)')  R, Z, A, BR, BZ, BA
           X = R * sin(A)
           Y = R * cos(A)
           write(2,fmt='(1p,6(e16.8),2(1x,i0))') Y,Z,X,BY,BZ,BX,ix,jr
         enddo
       enddo

       stop ' Job complete ! Field map stored in geneSectorMap.out.'
       end
```

Zgoubi optical sequence using `TOSCA`

```
A uniform field 180 degree sector dipole field map in cylindrical coordinates,
```

```
! used twice so to simulate a 360 degree cyclotron dipole.
! A 200 keV proton is tracked through. Its step-by-step coordinates are logged to zgoubi.plt.
 'OBJET'
64.62444403717985                                        ! Rigidity (kG.cm), 200keV proton.
2
1 1
12.9248888074 0. 0. 0. 0. 1. 'm'            ! Injection radius (all other coordinates zero).
1

 'PARTICUL'              ! This is required only because we want to get the time-of-flight,
938.27208 1.602176487D-19 1.79284735 0. 0.    ! raytracing otherwise just requires rigidity.
! PROTON                                                ! An alternate way to define a proton.

 'FAISTORE'
zgoubi.fai   #End       ! #End tells where (at which subsequent labeled keyword), particle
1                       ! data are to be logged to zgoubi.fai.
 'TOSCA'                ! First 180 degree field map
0  2                    ! IL=2 here logs the step-by-step proton coordinates to zgoubi.plt.
1.  1. 1. 1.
HEADER_8
315 121 1 22.1 1.       ! IZ=1 -> 2D ; MOD=22 -> polar map ; .MOD2=.1 -> single map.
geneSectorMap.out
0 0 0
2                       ! 9*9 node grid for second order fiel interpolation.
1.                      ! 1 cm step size.
2
0. 0. 0. 0.
 'TOSCA'                ! Second 180 degree field map
0  2                    ! IL=2 here logs the step-by-step proton coordinates to zgoubi.plt.
1.  1. 1. 1.
HEADER_8
315 121 1 22.1 1.       ! IZ=1 -> 2D ; MOD=22 -> polar map ; .MOD2=.1 -> single map
geneSectorMap.out
0 0 0 0
2                       ! 9*9 node grid for second order fiel interpolation
1.                      ! 1 cm step size
2
0. 0. 0. 0.

 'FAISCEAU'  #End       ! Label '#End' tells 'FAISTORE' to log particle data here!
 'END'
```

1.5.2 *Optical sequence using texttttDIPOLE*

The cyclotron is defined using a mathematical model for the dipole field, a 60^o sector, here. This optical sequence can be copy-pasted to a Zgoubi input data file and run as it is.

```
Cyclotron, classical.
 'OBJET'
64.62444403717985                                ! 200keV
2
4 1
12.9248888074 0.  0.   0.   0.  1. 'm'           ! 200keV. R=Brho/B=*/.5
28.9070891209 0.  0.   0.   0.  2.23654451125 'm'   ! 1 MeV. R=Brho/B=*/.5
50.           0.  0.   0.   0.  3.86850523397 'o'   ! at RM  (B*rho=0.5*0.5=0.25T.m, 2.9885 MeV)
64.7070336799 0.  0.   0.   0.  5.0063899693  'M'   ! 5 MeV. R=Brho/B=*/.5
1 1 1 1

 'DIPOLE'
0
60. 50.
30.  5. 0. 0. 0.
0.  0.                                           ! EFB 1  hard-edge
4  .1455   2.2670  -.6395  1.1558  0. 0.  0.
30. 0.  1.E6  -1.E6  1.E6  1.E6
0.   0.                                          ! EFB 2
4  .1455   2.2670  -.6395  1.1558  0. 0.  0.
-30. 0.  1.E6  -1.E6  1.E6  1.E6
0. 0.                                            ! EFB 3
0  0.      0.      0.      0.      0. 0.  0.
0. 0.  1.E6  -1.E6  1.E6  1.E6 0.
4   10.
1.                  ! The smaller, the better the orbits close.
2  0. 0. 0. 0.      ! Could also be, e.g., 2 50. 0. 50. 0. with Y0 amended accordingly in OBJET
 'FAISCEAU'
 'FAISTORE'
 zgoubi.fai
 1
 'END'
```

Bibliography

[1] E.O.Lawrence and N.E.Edlefsen, Science 72, 376 (1930);
E.O.Lawrence and M.S. Livingston, Phys. Rev. 37 (1931), 1707; 38, 136, (1931); 40, 19 (1932)
[2] T. Kawaguchi et al., Design of the sector magnets for the RIKEN superconducting ring cyclotron, Proceedings of the 15th International Conference on Cyclotrons and their Applications, Caen, France.
http://www.nishina.riken.jp/facility/SRC_e.html
[3] H.A.Bethe and M.E.Rose, Phys. Rev. 54, 588 (1938)
[4] L.H.Thomas, *The Paths of Ions in the Cyclotron*, Phys. Rev. 54, 580, (1938)
[5] F. Chautard, *Beam Dynamics For Cyclotrons*, in *CERN Accelerator School*, Zeegse, The Netherlands, 24 May-2 June 2005.
[6] J. Le Duff, *Longitudinal beam dynamics in circular accelerators*, in *CERN Accelerator School*, Jyvaskyla, Finland, 7-18 September 1992.
[7] T. Stammbach, *Introduction to Cyclotrons*, in *CERN accelerator school, cyclotrons, linacs and their applications*, IBM International Education Centre, La Hulpe, Belgium, 28 April-5 May 1994.
[8] H. A. Enge, Deflecting magnets, in Focusing of Charged Particles, Vol. 1, A. Septier Ed., Academic Press (1967).
[9] G. Leleux, Circular accelerators, INSTN lectures, SATURNE Laboratory, CEA Saclay (Juin 1978). Some passages of the present document are inspired from these lectures.